



Development of screening assays and discovery of initial inhibitors of pneumococcal peptidoglycan deacetylase PgdA

Nhat Khai Bui^a, Samo Turk^b, Stephan Buckenmaier^{c,1}, Flint Stevenson-Jones^a, Benjamin Zeuch^a, Stanislav Gobec^b, Waldemar Vollmer^{a,*}

^a Centre for Bacterial Cell Biology, Institute for Cell and Molecular Biosciences, Newcastle University, Richardson Road, Newcastle upon Tyne NE2 4AX, United Kingdom

^b Faculty of Pharmacy, University of Ljubljana, Aškerčeva 7, 1000 Ljubljana, Slovenia

^c Proteom Centrum Tübingen, University of Tübingen, Auf der Morgenstelle 15, 72076 Tübingen, Germany

ARTICLE INFO

Article history:

Received 21 February 2011

Accepted 31 March 2011

Available online 8 April 2011

Keywords:

Peptidoglycan deacetylase

PgdA

Lysozyme resistance

Virtual screening

ABSTRACT

The essential cell wall peptidoglycan is the target of several components of the innate immune system and its disruption results in lysis of invading bacteria. The pathogen *Streptococcus pneumoniae* produces a peptidoglycan N-acetylglucosamine deacetylase, PgdA, to modify the peptidoglycan structure. The activity of PgdA contributes to the bacteria's resistance to lysozyme, which is an important antimicrobial factor of the human innate immune system. In this study we report on the activity of PgdA against natural and artificial substrates. We have also established a virtual high-throughput screening and a new enzyme assay to search for compounds inhibiting PgdA. Two compounds with IC₅₀ values in the micromolar range have been identified and they could serve as leads for the search of inhibitors of PgdA, an important pneumococcal virulence factor.

© 2011 Elsevier Inc. All rights reserved.

1. Introduction

Streptococcus pneumoniae (the pneumococcus) is one of the most important human pathogens and can cause infectious diseases like pneumonia, otitis media and meningitis [1]. The encapsulated, Gram-positive bacterium has a lancet-shape morphology which is maintained by the pneumococcal cell wall. A major element of the cell wall is the peptidoglycan that protects the cell against the internal osmotic pressure. Peptidoglycan consists of glycan chains of alternating β 1,4-linked N-acetylglucosamine (GlcNAc) and N-acetylmuramic acid (MurNAc) residues that are cross-linked by oligopeptides [2]. The peptidoglycan hydrolase lysozyme is widely present in animals, plants, fungi and bacteria and is an important bacteriolytic component of the human

innate immune system. Lysozyme hydrolyses the glycosidic bonds within the peptidoglycan glycan chains causing disintegration of the peptidoglycan structure and thereby lysis of the cell. In *S. pneumoniae* and other pathogens the glycan chains become modified shortly after their synthesis by O-acetylation (of MurNAc) and de-N-acetylation (MurNAc and/or GlcNAc) [3–5]. These modified glycan chains are poor substrates for lysozyme thereby contributing to the resistance to this antimicrobial enzyme [6]. Peptidoglycan deacetylation is catalyzed by the peptidoglycan N-acetylglucosamine deacetylase A (PgdA) and affects 30–80% of the GlcNAc residues. The *pgdA* gene was first identified in *S. pneumoniae* [5] and has since been reported to be present in many other species including *Bacillus subtilis* [7], *Bacillus cereus* [8], *Lactococcus lactis* [9], *Streptococcus mutans* [10], *Listeria monocytogenes* [11,12] and *Enterococcus faecalis* [13]. Furthermore, zoonotic pathogens such as *Streptococcus suis* [14] and *Streptococcus iniae* [15] that have a significant influence on industrial livestock and aquaculture production have also been reported to have peptidoglycan deacetylase. Mutants from human and animal pathogenic strains lacking the peptidoglycan deacetylase gene are significantly impaired in their virulence [6,11–15]. Interestingly, in *S. suis* the *pgdA* gene is expressed at low level under laboratory conditions and is up-regulated during infection in the pig host organism [14].

The crystal structure of pneumococcal PgdA (SpPgdA) has elucidated the catalytic mechanism of peptidoglycan deacetylation and the kinetic parameters of SpPgdA were determined using GlcNAc₃ as a substrate [16]. The peptidoglycan deacetylases

Abbreviations: PG, peptidoglycan; GlcNAc, N-acetylglucosamine; MurNAc, N-acetylmuramic acid; PgdA, peptidoglycan N-acetylglucosamine deacetylase A; IC₅₀, half maximal inhibitory concentration; IPTG, isopropyl- β -D-thiogalactopyranoside; CTAB, cetyltrimethylammonium bromide; GlcNAc₅, N,N,N,N,N-pentaacetylchitopentaose; pNPA, p-nitrophenyl acetate; α NAO, -naphthyl acetate; 4MUA, 4-methylumbelliferyl acetate; DMSO, dimethylsulfoxide.

* Corresponding author at: Centre for Bacterial Cell Biology, Medical School, University of Newcastle upon Tyne, Baddiley Clark Building, Richardson Road, Newcastle upon Tyne NE2 4AX, United Kingdom. Tel.: +44 0 191 208 3216; fax: +44 0 191 208.

E-mail address: W.Vollmer@ncl.ac.uk (W. Vollmer).

¹ Present address: Agilent Technologies, Hewlett Packard Strasse 8, 76337 Walddbronn, Germany.

BC1960 and BC3618 from *B. cereus* are active against peptidoglycan of *B. subtilis* and *H. pylori* [8]. More recently, PgdA from *L. monocytogenes* has been shown to be able to release acetate from *Listeria* peptidoglycan and to deacetylate GlcNAc [12]. The growth and morphology of the *L. monocytogenes* *pgdA* mutant resembled those of the parental strain. However, the mutant was more susceptible to lysozyme or muramidases and was more prone to EDTA- or Triton X-100-induced autolysis.

PgdA is a validated antibiotic target as demonstrated by the reduced virulence of mutant strains of various pathogens [6,11–15]. Thus, antibiotic inhibition of PgdA would enable the host organism to lyse invading bacteria with lysozyme that is inactive against bacteria with functional PgdA. However, to date no enzyme inhibitor has been published for this protein. In this study we present evidence of an *in vitro* deacetylase activity of PgdA against *S. pneumoniae* peptidoglycan and other substrates. We have developed a simple microtiter-based activity assay with chromogenic substrates. We have used the assay to screen for potential PgdA inhibitors selected by computational virtual-screening. Two of the inhibitors identified had IC₅₀ values in the micromolar range.

2. Experimental procedures

2.1. Materials

All Chemicals were purchased from Sigma (Munich, Germany) unless indicated otherwise. 96-well plates (ref. 655101) from Greiner bio-one (Frickenhausen, Germany) were used for the screening assays. Cellosyl was provided by Hoechst AG, Frankfurt, Germany.

2.2. Preparation of chemically acetylated, tritiated peptidoglycan

Cell wall from *S. pneumoniae* strain R36A was prepared as described [6]. Twelve mg of cell wall was suspended in 1.2 ml of water and stirred for 30 min at ambient temperature. The sample was cooled with ice and 750 μ l of saturated NaHCO₃ solution and 1 ml of 5% freshly prepared, [³H]-labelled acetic anhydride (total 25 mCi) were added and the sample was stirred on ice for 30 min. After the addition of 0.5 ml of 5% unlabelled acetic anhydride the sample was stirred for 30 min on ice and for 1 h at ambient temperature. Thirty ml of water was added and the acetylated cell wall was collected by centrifugation (25,000 \times g, 30 min, 4 °C), washed with 6 \times 30 ml of water and dried in a SpeedVac. To remove wall teichoic acid 3.5 mg of [³H]-labelled cell wall was incubated with 48% hydrofluoric acid for 48 h at 4 °C. The resulting tritiated peptidoglycan was washed as described [6] and had a specific activity of 5.67 \times 10⁶ dpm/mg.

2.3. Cloning of the *pgdA* gene

Part of the *pgdA* gene (nucleotides 735–1389) was amplified from DNA from *S. pneumoniae* R36A using standard polymerase chain reaction (PCR) procedures. The following oligonucleotides (Biomers, Ulm, Germany) were used:

(PgdA735) TCA CATATG ATC CAA TCT TCG TAC TTA CTC and PgdA(1389) CCA GAATTC GTC TGT CAA ATA TCT AAC CAG (NdeI and BamHI restriction sites underlined).

The PCR products were digested with NdeI and BamHI (Fermentas, St. Leon-Rot, Germany) and ligated into pET14b plasmid (Novagen, Darmstadt, Germany) digested with the same restriction enzymes. This cloning strategy introduced an N-terminal His-tag. After transformation into *E. coli* XL1-Blue the plasmid was isolated and transformed into the expression strain *E. coli* BL21(DE3) pLysS resulting in strain BL21 (DE3) pLysS pET14b-*pgdA*(735–1389). The product is a truncated PgdA version which

lacks the signal peptide and the N-terminal non-catalytic domain. It contains part of the middle domain and the catalytic C-terminal domain and has the sequence MGSHHHHHHSSGLVPRGSHM-PgdA^{245–463} (numbers are according to amino acid sequence). Upon cleavage with thrombin the recombinant protein has the sequence GSHM-PgdA^{245–463} and is designated PgdA^{245–463} in the following sections.

2.4. Protein purification

BL21 (DE3) pLysS pET14b-*pgdA*(735–1389) was inoculated into 400 ml of LB medium containing chloramphenicol (34 μ g/ml) (Serva, Heidelberg, Germany) and ampicillin (50 μ g/ml) (Boehringer, Mannheim, Germany) and incubated at 37 °C to an A₅₇₈ of 0.6. The cells were harvested by centrifugation (20 min, 8300 g) and resuspended in 400 ml LB medium. Isopropyl- β -D-thiogalactopyranoside (IPTG) was added to a final concentration of 0.4 mM to induce the expression of *pgdA*(735–1389) and the cells were incubated for a further 3 h. The cells were harvested by centrifugation and resuspended in 25 mM Tris/HCl buffer, pH 7.5, 100 mM NaCl (buffer 1).

DNase (0.5–1 mg) and 1 mM PMSF were added before cell disruption by French press (AIC, Silverspring Maryland, USA) (700 psi). The soluble fraction was collected by centrifugation (90 min, 29,600 \times g) and was incubated with Co-affinity beads (TalonTM, Clontech, Mountain View, USA) at 4 °C for 2 h on a vertical rotating device at 4 °C. The beads were transferred to a column and washed with 20 mM Tris/HCl pH 7.5, 0.5 M NaCl, 10 mM imidazole followed by elution of the protein with 20 mM Tris/HCl pH 7.5, 0.5 M NaCl, 200 mM imidazole. The protein was dialysed for 18 h against buffer 1 containing 10 units of Thrombin (Novagen, Germany) to remove the oligo-His-tag. The protein purity and completeness of thrombin cleavage were verified by sodium dodecyl sulfate-polyacrylamide gel electrophoresis (SDS-PAGE) (Supplemental Fig. 1).

2.5. Enzyme assays

Different substrates were used in assays with PgdA^{245–463}. The samples contained 1 μ M enzyme and 5 μ M CoCl₂ and had a total volume of 100 μ l. The incubation temperature was 37 °C.

The enzyme activity was determined with chemically [³H]acetylated peptidoglycan (total radioactivity used in each assay was 65,000 dpm) from *S. pneumoniae* R36A in 25 mM Tris-maleate, pH 5.0 (buffer A), 25 mM Tris/HCl, pH 7.0 (buffer B), 25 mM Tris/HCl, pH 8.0 (buffer C) or 25 mM sodium borate, pH 9.5 (buffer D). The reaction was terminated by the addition of 100 μ l 0.2 M HCl and 5 μ l 1 M acetic acid. Acetic acid was extracted with 500 μ l ethyl acetate and radioactivity in the organic phase was measured by scintillation counting.

For testing the maximal release of acetate from the [³H]acetylated peptidoglycan from *S. pneumoniae* R36A the reaction was performed in 25 mM Tris/HCl pH 7.0 in a total volume of 400 μ l. After 24 h one quarter of the sample was added to 100 μ l 1% cetyltrimethylammonium bromide (CTAB) and incubated for 20 min on ice to precipitate the high-molecular weight peptidoglycan. The mixture was centrifuged (20 min, 16,000 \times g) and the radioactivity present in 100 μ l of the supernatant was quantified by scintillation counting. The remaining of the sample was split into 3 aliquots that received either another 1 μ M of enzyme, 5 μ l of peptidoglycan (13,000 dpm/ μ l) or nothing. After 24 h of further incubation the peptidoglycan was precipitated as described above and the radioactivity in the supernatant was measured.

PgdA activity was also tested with cell wall, peptidoglycan and mucopeptides from *S. pneumoniae*; peptidoglycan and mucopeptides from *E. coli*, cell wall from *S. aureus* and from *S. carnosus*, and

N,N,N,N,N-pentaacetylchitopentaose (GlcNAc₅) as possible substrates. The incubation was performed in 25 mM Tris/HCl, 5 μ M CoCl₂ pH 7.0. Muropeptides and GlcNAc₅ were incubated for 2 h, while cell wall or peptidoglycan was incubated for 16 h. The samples were analysed by HPLC and fractions collected were analysed by mass spectrometry (see below). Cell wall, peptidoglycan and muropeptides from *S. pneumoniae*, cell wall from *S. aureus* and *S. carnosus* were analysed by HPLC as described [17]. Peptidoglycan and muropeptides from *E. coli*, the muropeptides from *S. aureus* and GlcNAc₅ were analysed as described [18].

2.6. Mass spectrometry

HPLC fractions of muropeptides were desalted using ZipTip C18 pipette tips (Millipore, Schwalbach, Germany). The samples were eluted with 4 μ l 0.5% acetic acid and an aliquot of 0.5 μ l was applied on a metal well-plate coated with α -cyano-hydroxy-nitrocellulose. MALDI-TOF analysis was performed on the Reflex III Mass Spectrometer (Bruker, Bremen, Germany) using XACQ 4.0 software. The data was processed using the software XMASS 5.1. Offline electrospray MS was performed as published [19].

2.7. Determination of the kinetic parameters

Samples contained 1 μ M enzyme and 5 μ M CoCl₂ and had a total reaction volume of 100 μ l. The assay buffer was either 25 mM Tris/HCl pH 7.0 (buffer B) or 25 mM Tris/HCl pH 8.0 (buffer C). The kinetic parameters were determined with p-nitrophenyl acetate (pNPA) and 4-methylumbelliferyl acetate (4MUA). The substrate concentrations ranged from 2 to 10 mM for pNPA and 0.2 to 1.0 mM for 4MUA, which is below the K_m values (Table 1), due to their insufficient solubility. The assays were performed in buffer B, 10% DMSO in a 96-well microtiter plate for 30 min at 37 °C. The kinetic property of 4MUA was also determined in buffer C. The reaction progress was monitored in a Spectra-Max 340 PC (Molecular Devices, Sunnyvale, CA, USA) microplate reader at 405 nm for the pNPA assay and at 354 nm for the 4MUA assay. The kinetic parameters K_m and V_{max} were determined by fitting the data to the Michaelis–Menten equation by non-linear regression using the Prism 5 software (GraphPad Software, La Jolla, CA, USA).

2.8. Compound screen

The inhibitor screen was performed in 25 mM Tris/HCl pH 7.0 at 37 °C for 15 min using 1 mM 4MUA as a substrate and 1 μ M Pgda^{245–463} enzyme with or without 1 mM compound dissolved in DMSO. The total volume was 100 μ l with a final concentration of 10% DMSO. Some samples contained 0.01% Triton X-100. Reactions were monitored with the BMG Labtech FluoStar Optima microtiter plate reader. The excitation wavelength was 355 nm and the emission wavelength was 460 nm.

2.9. Computer-aided virtual high-throughput screening to identify potential inhibitors of Pgda

Computational part was done on workstation with 4 dual core AMD Opteron 2.0 GHz processors, 16 GB of RAM, 4 320 GB hard

drives in RAID10 array and nVidia GeForce 7900 graphic card. Workstation has Fedora 7 64bit installed.

For initial virtual screening the American National Cancer Institute (NCI) bank of 280,000 compounds was selected. Due to the size of NCI bank of compounds, filtering procedure was applied first to eliminate compounds with unwanted properties. Filtering was based on simple molecular descriptors and was done with program Filter (OpenEye Scientific Software Inc). Choice of descriptors was based loosely on Lipinski rule of five [20]: molecular weight: 200–600 g/mol, number of ring systems: 1–5, number of hetero atoms: 4–20, number of H-bond donors: 0–6, number of H-bond acceptors: 0–14; log *P*: –3.0 to 4.0. Additional filters were used to eliminate insoluble compounds (set to moderate), to eliminate all the compounds with atoms other than H, C, N, O, F, S, Cl and Br, and to eliminate all the compounds with reactive functional groups. Also a function developed by Shoichet, implemented in the program Filter, that eliminates known aggregators and also removes the predicted aggregators was used [21]. Using this function we anticipate eliminating potential promiscuous inhibitors. Result of filtering was a new subset of compounds containing roughly 55,000 structures.

For docking experiment, FlexX 3.1. (BioSolveIT GmbH) [22] was used on the crystal structure of Pgda from *S. pneumoniae* co-crystallized with acetate (PDB entry: 2C1G) [16]. The active site was defined as an area of the enzyme within 7.5 Å from the co-crystallized acetate. The co-crystallized zinc bound in zinc finger was left in the active site and octahedral coordination was selected. Water 176 was defined as freely rotatable and displaceable so that it can bridge H-bonds if possible, if not FlexX ignores it. Protonations of amino acids and orientations of H-bond donors were setup manually. Since zinc ion is an important part of the active site, docking experiment was set up in such manner that it considers only the solutions that predict the binding of compounds with zinc ion. For base placement Triangle Matching was used and the program generated maximally 200 solutions per iteration and 200 per fragmentation.

All of the 55,000 compounds were then docked in the active site of Pgda and ranked according to their scores. 40 of the best compounds were selected and ordered from NCI, 2 were out of stock and 38 compounds were tested *in vitro* (Supplemental Table 1). After obtaining *in vitro* results, a 3D similarity search was performed to obtain compounds similar to the most active compound 2. This time, the combined bank of compounds from suppliers ChemBridge, Maybridge, Asinex and NCI, containing 1.8 million structures, was used. 3D Similarity search was done with ROCS (OpenEye Scientific Software Inc.) [23]. Additionally, LIQUID plugin for PyMol [24] was used to visualize pharmacophoric features of query compound 2 and only the compounds with the same features were selected. Finally, 9 compounds (compounds 3–11) with similar volume, shape and pharmacophoric features as compound 2 were selected and purchased.

3. Results

3.1. Pgda activity against the oligosaccharide GlcNAc₅

We have purified from *E. coli* a recombinant, soluble version of Pgda, Pgda^{245–463}, containing an N-terminal His₆-tag, by Co²⁺-affinity chromatography. Pgda^{245–463} consists of the catalytic C-terminal domain and part of the middle domain. The oligohistidine tag was removed by cleavage with thrombin (Fig. S1). We found that Pgda^{245–463} was able to de-acetylate the GlcNAc₅ (Fig. 1A) but not GlcNAc (not shown). GlcNAc₅ was almost quantitatively converted to mono-, di- and tri-de-acetylated products as shown by HPLC and MALDI-MS analysis of the products (Fig. 1).

Table 1
Activity of Pgda^{245–463} against artificial substrates.

(pH value)	K_m [mM]	V_{max} [μ mol/min/mg]	k_{cat} [s^{-1}]	k_{cat}/K_m [$M^{-1}s^{-1}$]
pNPA	16.74 \pm 7.11	1.11 \pm 0.30	0.46 \pm 0.12	28.8
4-MUA (pH 7.0)	2.27 \pm 1.20	0.68 \pm 0.27	0.28 \pm 0.11	129
4-MUA (pH 8.0)	2.38 \pm 0.67	3.95 \pm 0.66	1.64 \pm 0.27	710

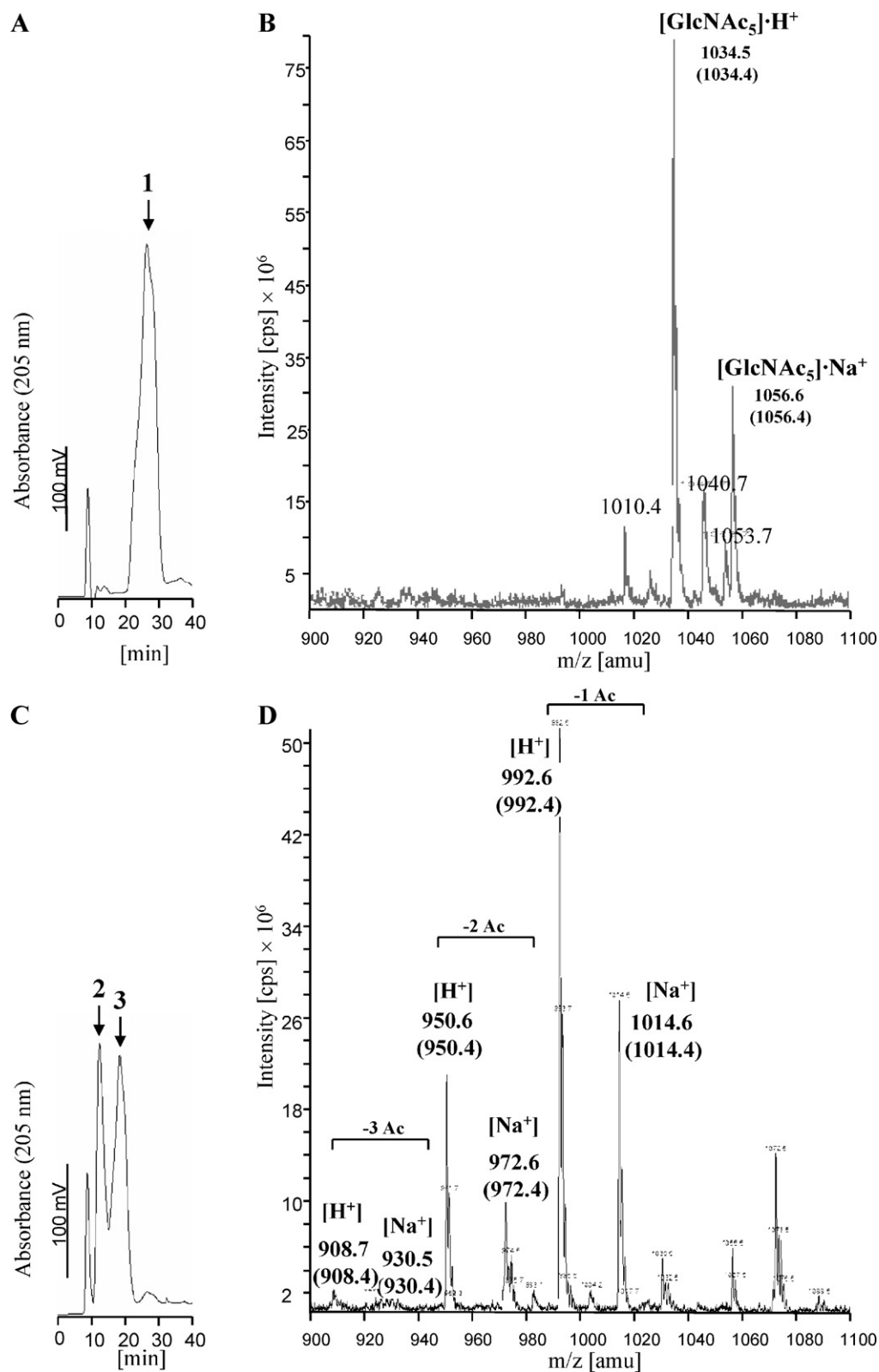


Fig. 1. Deacetylation of GlcNAc₅ by Pgda^{245–463}. HPLC profiles (A and C) and MALDI mass spectra (positive ion mode) (B and D) of GlcNAc₅ (A and B) and its products upon incubation with Pgda^{245–463} (C and D). (A) GlcNAc₅ eluted at 25 min (arrow 1). (B) Mass spectrum of GlcNAc₅ with the masses of the H⁺ and Na⁺ forms. The numbers in brackets indicate the theoretical masses. (C) GlcNAc₅ was incubated with Pgda^{245–463} followed by HPLC analysis. The two new peaks (arrows 2 and 3) correspond to deacetylated products of GlcNAc₅. (D) The combined fractions of peaks 2 and 3 (C) were analysed by mass spectrometry. The Pgda^{245–463} products lacked 1, 2 or 3 acetyl groups (theoretical masses in brackets).

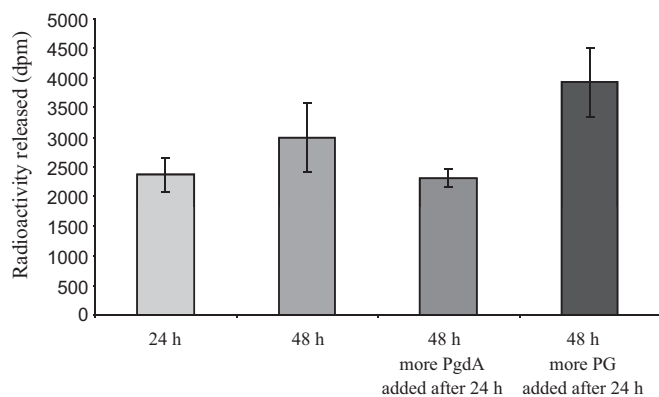


Fig. 2. Release of radioactive acetate from pneumococcal cell wall by PgdA^{245–463}. The time of incubation and the addition of more enzyme or substrate is indicated below the columns. The values are mean \pm SD of two independent samples. The total radioactivity was 65,000 dpm. PgdA^{245–463} maximally released \sim 4% of the total radioactivity of chemically acetylated peptidoglycan.

3.2. PgdA activity against peptidoglycan and muropeptides

We have next assayed the activity of PgdA against peptidoglycan or peptidoglycan fragments (muropeptides) isolated from different bacterial species. The first substrate we tested was peptidoglycan from wild-type *S. pneumoniae* that has been chemically N-acetylated with ³H-labelled acetic anhydride. PgdA^{245–463} was able to release a small fraction (\sim 4%) of the radioactive acetate from this substrate (Fig. 2). We would expect to obtain a low percentage of radioactivity release from this substrate because (i) a large proportion (30–50%) of naturally acetylated GlcNAc residues were not labelled and thus their deacetylation is not detectable by the method, and (ii) the chemical acetylation most likely also labels the primary amino groups in the peptide part that cannot be deacetylated by PgdA. In addition, the low percentage of acetate release could be due to a limited number of acetate residues being susceptible to the enzyme or due to the inactivation of the enzyme during the period of the reaction. To test these possibilities we added either a second aliquot of acetylated cell wall or more enzyme at the end of the reaction followed by a second period of incubation. The addition of more enzyme could not release more acetate, whereas more acetate was released upon addition of more peptidoglycan substrate (Fig. 2). We concluded that a limited fraction of GlcNAc residues in chemically acetylated pneumococcal peptidoglycan is prone to deacetylation by PgdA.

Peptidoglycan from wild-type *S. pneumoniae* contains a fraction of de-acetylated glucosamine residues. When the peptidoglycan was incubated with PgdA^{245–463} the percentage of deacetylation did not further increase indicating that the residual GlcNAc residues are not accessible to the enzyme (Fig. 3A). Interestingly, PgdA^{245–463} was active against peptidoglycan isolated from the *pgdA* mutant strain, which does not contain glucosamine residues (Fig. 3B, [5]), demonstrated by the presence of 7–21% deacetylated muropeptides in the cellosyl-digested peptidoglycan (Fig. 3B). MS and MS/MS analysis confirmed that one of the muropeptides generated by PgdA corresponded to the deacetylated version of the major monomeric muropeptide, Tri(deAc) (Fig. 3D). PgdA^{245–463} was also active against peptidoglycan from *S. suis*, which has similar basic structure as that from *S. pneumoniae*, but was inactive against peptidoglycans from *S. aureus*, *S. carnosus* or *E. coli* that have different peptide structure than peptidoglycan from *S. pneumoniae*. PgdA^{245–463} was inactive against soluble muropeptides from the *S. pneumoniae pgdA* mutant strain (Fig. 3C) and from other species (not shown). These data confirm that PgdA^{245–463} has the ability to release *in vitro* a limited number of acetate residues

from pneumococcal peptidoglycan, but not from other species, and that it deacetylates the high-molecular weight substrate but not small, soluble peptidoglycan fragments. The limited activity of PgdA^{245–463} against natural substrates was not due to the absence of the N-terminal domain because a soluble version comprising the N-terminal domain and lacking the signal peptide, PgdA^{39–463}, did not have higher activity than PgdA^{245–463} (data not shown).

3.3. Enzyme activity against chromogenic substrates and development of an assay for inhibitor screening

Having demonstrated deacetylase activity against natural substrates we aimed to develop a simple enzyme assay for screening of inhibitors. For this we have tested various possible chromogenic substrates of PgdA. Indeed, we found that PgdA^{245–463} released acetate from p-nitrophenyl acetate (pNPA) or 4-methylumbelliferyl acetate (4MUA). The assays were performed at pH 7.0 for all chromogenic substrates used. For 4MUA the assay was also carried out at pH 8.0. The enzyme reaction for these chromogenic substrates followed the steady-state kinetics described by the Michaelis-Menten equation. The kinetic parameters K_m and V_{max} were determined by non-linear regression (Table 1). PgdA^{245–463} had the highest k_{cat}/K_m value with 4MUA ($128.61 \text{ M}^{-1} \text{ s}^{-1}$) compared to the pNPA. With 4MUA as substrate the enzyme exhibited a ca. 6-fold higher k_{cat}/K_m value at a pH of 8.0 as compared to pH 7.0.

3.4. Discovery of a new potential inhibitor of PgdA by computational virtual screening and *in vitro* assay

Virtual screening was done on NCI bank of 280,000 compounds which was filtered to loosely comply with the Lipinski rule of five [20]. The remaining 55,000 compounds were then docked in PgdA active site using FlexX [22]. PgdA has well defined active site with typical zinc finger. Zinc ion is complexed by two histidines (His326 and His330) and aspartic acid (Asp276) (Fig. 4A). This structural feature is conserved throughout CE-4 family of enzymes. In addition to amino acid residues mentioned above, water 176 and acetate (product of the reaction catalyzed by PgdA) coordinate zinc in octahedral coordination. Acid-base catalysis is performed by two charge relay pairs. One is formed by Asp275 and Arg664 and the other by His417 and Asp 391. Zinc bound water 176 functions as a nucleophile [16]. For docking experiment the active site was defined as an area of the enzyme within 7.5 Å from the co-crystallized acetate. All 55,000 pre-filtered compounds were docked and 40 compounds with best scores were ordered from NCI. 38 available compounds were tested in *in vitro* assay (Supplemental Table 1). Two compounds showed promising inhibitory activities: compound 1 had an IC_{50} value of 638 μM and compound 2 an IC_{50} value of 132 μM . We determined the inhibitory activity of compound 2 also in presence of 0.01% of Triton X-100 and it remained unchanged confirming nonpromiscuous mode of inhibition [21].

Our docking study shows that compound 2 complexes zinc with the carboxylic and keto functional groups (Fig. 4B). The carboxylic group is placed at the same position as acetate in the crystal structure 2C1G.pdb, while the keto group replaces water 176. The keto group also forms an additional interaction with His417, while the aromatic hydroxyl group forms a H-bond with Asp276.

In order to find additional inhibitors with structures related to compound 2, 3D similarity search was performed which involved the complete NCI bank of compounds and some commercially available banks of compounds. 3D similarity search was done with the program ROCS [23]. Results were then visualized with PyMol and only compounds that comply to pharmacophoric model (Fig. 4C) were selected. Nine structurally related compounds were

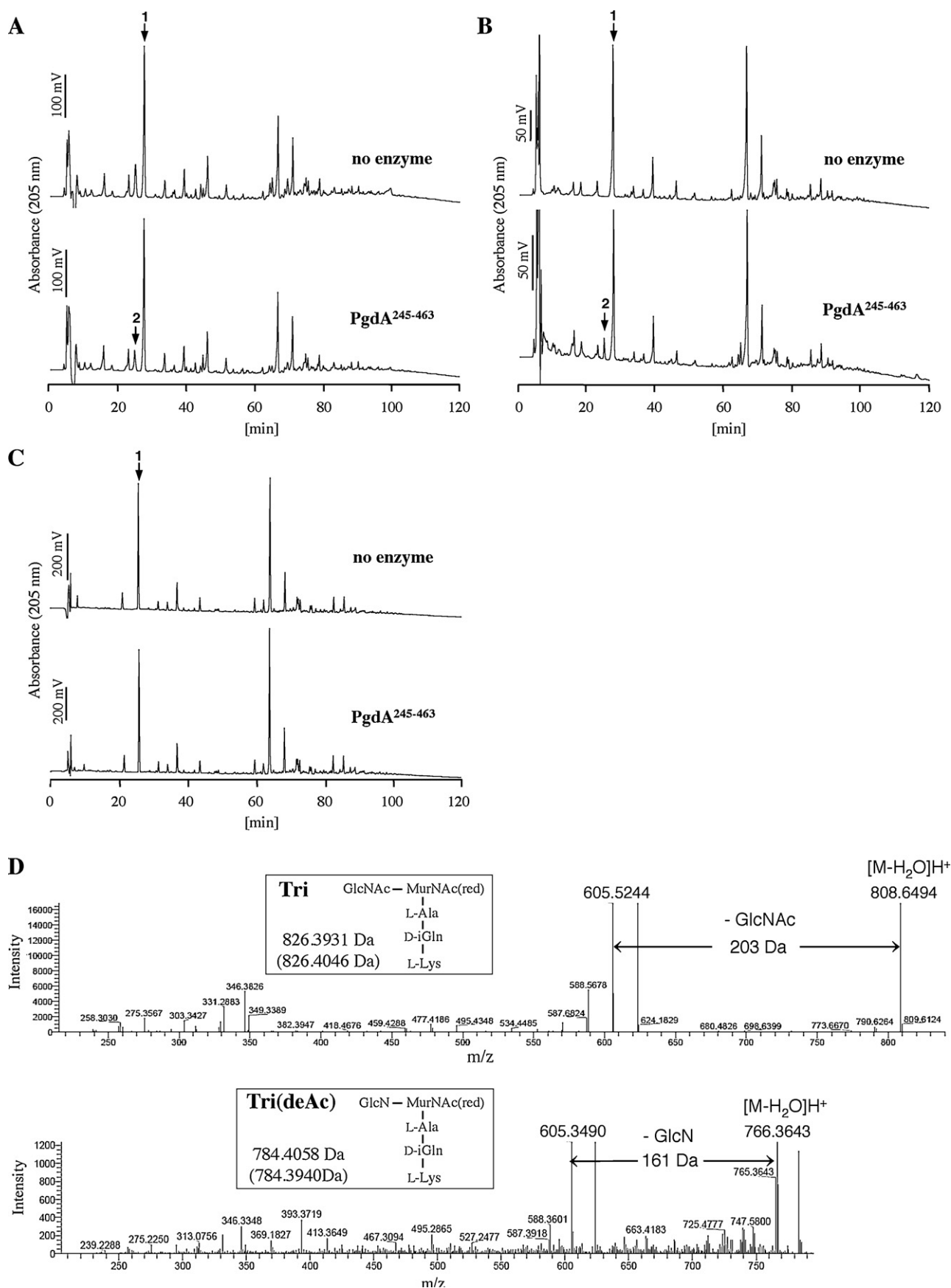


Fig. 3. Deacetylation of pneumococcal peptidoglycan by Pg dA^{245–463}. Peptidoglycan from *S. pneumoniae* wildtype (A), peptidoglycan from the *pgdA* mutant strain (B) or muropeptides from the *pgdA* mutant strain (C) was incubated with or without Pg dA^{245–463}. Peptidoglycan samples were digested with cellosyl, and all samples were reduced with sodium borohydride and analysed by HPLC. (D) MS/MS spectra of the major muropeptide Tri (GlcNAc–MurNAc–L-Ala–D-iGln–L-Lys) (top) and its deacetylated version

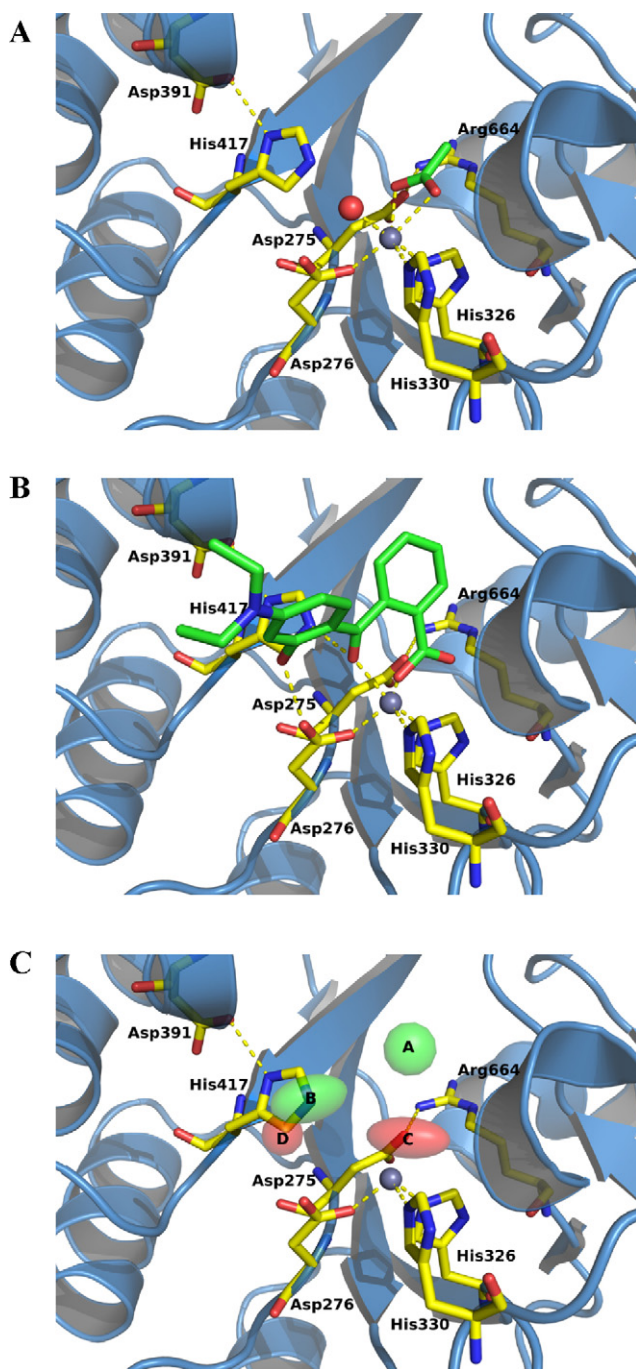


Fig. 4. Active site of PgdA. (A) Only important amino acid residues of the active site of PgdA are shown as yellow sticks. The rest of the enzyme is shown as blue cartoon. The zinc ion is shown as gray sphere, water 176 is shown as red sphere and acetate is shown as green sticks. All relevant interactions are shown as yellow dashes. (B) Compound 2 (green) docked in the active site of PgdA. Interactions with active site amino acid residues and zinc ion are shown as green dashes. (C) Pharmacophore model of structural features needed for inhibition of PgdA. Regions A and B represent two aromatic rings. Region C represents functional groups that can interact with the zinc ion and region D represents functional groups interacting with Asp276.

found; however, none of them exhibited better inhibitory activity than the parent compound 2 (compounds 3–11, Table 2).

4. Discussion

The peptidoglycan-specific sugar *N*-acetylmuramic acid is GlcNAc with a lactoyl residue at C3 and so the poly-(GlcNAcMurNAc) glycan strand backbone of peptidoglycan is chemically similar to linear oligo-GlcNAc chains, i.e. soluble *N*-acetylchitooligomers. It is therefore not surprising that the peptidoglycan deacetylase PgdA is related to chitin deacetylases and to nodulation factors that work on oligo-GlcNAc substrates. Moreover, PgdA from *S. pneumoniae* has been shown to deacetylate GlcNAc₃ [16] and two homologs from *B. cereus* were active against GlcNAc_{2–6}, with highest activity against GlcNAc₄ [8]. Both *B. cereus* enzymes were inactive against monomeric GlcNAc, whereas PgdA from *L. monocytogenes* was capable of deacetylating GlcNAc as detected by mass spectrometry analysis [11]. Our data confirmed an activity of *S. pneumoniae* PgdA against GlcNAc₅, which was deacetylated to the mono-, di- and tri-deacetylated compounds by the enzyme, and like in the case of the *B. cereus* enzymes we were unable to detect an activity against monomeric GlcNAc. Together these data suggest that the *S. pneumoniae* and *B. cereus* enzymes are capable of deacetylating only a limited number of GlcNAc residues in oligo-GlcNAc chains but this might not be a general property of PgdA deacetylases.

There are few reports on the activity of PgdA enzymes on natural substrates. Two *B. cereus* PgdA homologs BC1960 and BC3618 deacetylated the mucopeptide GlcNAc-MurNAc-L-Ala-D-Gln as well as peptidoglycan from *H. pylori* [8] although *H. pylori* peptidoglycan contains different peptides than that of *B. cereus*. *S. pneumoniae* PgdA was active against pneumococcal peptidoglycan, as shown in this work by the release of radioactive acetate and by the HPLC/MS-detection of deacetylated mucopeptides obtained from a PgdA-treated peptidoglycan sample of a *pgdA* mutant strain. The extent of deacetylation *in vitro* was lower than that observed in peptidoglycan from wt cells indicating that the enzyme is more active in the cell, perhaps due to its membrane-location in proximity of the newly made peptidoglycan or due to the stimulatory effects of cellular components not present in the *in vitro* system. Interestingly, PgdA was neither active against soluble peptidoglycan fragments, i.e. the mucopeptides, nor against peptidoglycan from other bacterial species. The structural basis for this specificity remains to be determined.

PgdA had a higher catalytic efficiency at pH 8.0 as compared to pH 7.0 with 4MUA substrate (Table 1). Based on the suggested reaction mechanism for pneumococcal PgdA [16] it is possible that the abstraction of a proton from the Zn²⁺-bound water molecule by Asp275, which initiates the reaction, is more efficient at pH 8.0 than at pH 7.0, but this hypothesis requires further testing. Notably, previous work showed different pH optima for two peptidoglycan deacetylases from *B. cereus*. BC1960 has a pH optimum at pH 6.0, BC3618 at pH 8.0 [8] and the reason for this difference is not known.

Virtual screening methods are increasingly used to identify potential new lead compounds in drug discovery [25,26] and have also been successfully used on antibacterial targets [27]. To date no inhibitor of PgdA has been published. Using computational structure-based virtual screening followed by biochemical evaluation, we were able to identify two promising inhibitors of PgdA, compounds 1 and 2 (Table 2), with IC₅₀ values of 584 μM and 130 μM, respectively. Our enzyme assays developed could also be

Tri(deAc) (bottom) obtained from HPLC fractions 1(Tri) and 2 [Tri(deAc)] of the chromatograms shown in B. The mass difference corresponding to loss of either GlcNAc or GlcN from the [M–H₂O]H⁺ ion is shown on the right side. The insets show the structure of the mucopeptide and the determined neutral mass. The theoretical mass is given in brackets.

Table 2Inhibitory effect of compounds on PgdA^{245–463}.

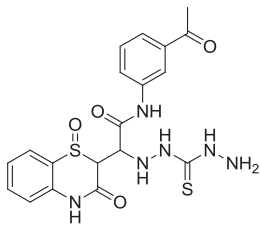
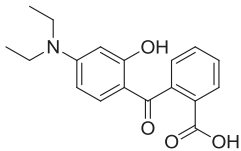
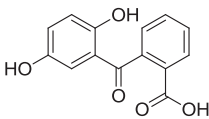
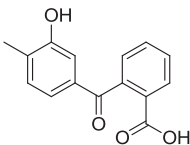
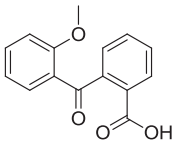
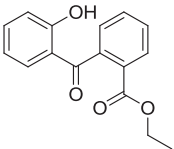
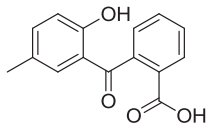
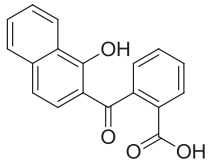
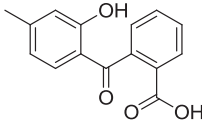
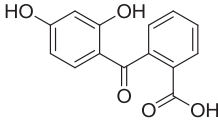
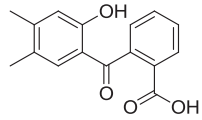
Compound ^a	Structure	% Residual enzyme activity at 1 mM	IC ₅₀ (μM)
1 (NSC648612)		29 ± 4.2	584 ± 115
2 (NSC625797, CH5472223) ^b		7 ± 1.4(5.9 ± 0.2) ^c	130 ± 20
3 (NSC37427)		123.0 ± 0.4	
4 (NSC159284)		62.3 ± 1.1	
5 (NSC338406)		66.4 ± 0.5	
6 (NSC400732)		75.8 ± 0.8	
7 (NSC407886)		62.5 ± 0.9	
8 (CH5475540)		51.3 ± 0.8	

Table 2 (Continued)

Compound ^a	Structure	% Residual enzyme activity at 1 mM	IC ₅₀ (μM)
9 (CH5626971)		93.8 ± 1.1	
10 (CH5629492)		33.7 ± 0.5	
11 (CH5944694)		53.0 ± 0.2	

^a Compounds with NSC numbers were obtained from NCI, compounds with CH numbers were obtained from ChemBridge.

^b Compound was obtained from two different suppliers.

^c Number in brackets: assay contained 0.01% Triton X-100.

used for high-throughput screening. The more potent inhibitor 2 was selected as a starting point for further computational similarity search in order to rapidly identify a series of structurally related compounds. Although this similarity search did not yield more potent inhibitors, it provided some insight into which structural elements are beneficial for inhibition of PgdA within this series. Compounds 2–11 share a common 2-benzoylbenzoic acid scaffold with different substituents on benzoyl part of the molecule and all except compounds 3 and 9 show some inhibitory activity. Substitution on the position 4 of the benzoyl part appears to be of significant importance for inhibitory activities of compounds with diethylamino substituent (compound 2) being the most promising. In order to find inhibitors with improved PgdA inhibitory activities, we propose to use compound 2 as a starting point for further medicinal chemistry efforts. We propose the synthesis of extended series of structurally related compounds where 2-(4-(diethylamino)benzoyl)benzoic acid is retained and different substituents are systematically introduced to various positions of both aromatic rings.

Acknowledgements

We thank Daniela Vollmer and Alice Eberhardt for cell wall from *S. pneumoniae*, Teresa de Almeida Figueiredo for cell wall from *S. aureus*, Jacob Bilboy for the critical reading of the manuscript and OpenEye Scientific Software Inc. for free academic licenses of their software. This work was supported by the European Commission through the EUR-INTAFAR project.

Appendix A. Supplementary data

Supplementary data associated with this article can be found, in the online version, at [doi:10.1016/j.bcp.2011.03.028](https://doi.org/10.1016/j.bcp.2011.03.028).

References

- [1] Weiser JN. The pneumococcus: why a commensal misbehaves. *J Mol Med* 2010;88:97–102.
- [2] Vollmer W, Blanot D, de Pedro MA. Peptidoglycan structure and architecture. *FEMS Microbiol Rev* 2008;32:149–67.
- [3] Crisostomo MI, Vollmer W, Kharat AS, Inhülsen S, Gehre F, Buckenmaier S, et al. Attenuation of penicillin resistance in a peptidoglycan O-acetyl transferase mutant of *Streptococcus pneumoniae*. *Mol Microbiol* 2006;61:1497–509.
- [4] Vollmer W. Structural variation in the glycan strands of bacterial peptidoglycan. *FEMS Microbiol Rev* 2008;32:287–306.
- [5] Vollmer W, Tomasz A. The pgdA gene encodes for a peptidoglycan N-acetylglucosamine deacetylase in *Streptococcus pneumoniae*. *J Biol Chem* 2000;275:20496–501.
- [6] Vollmer W, Tomasz A. Peptidoglycan N-acetylglucosamine deacetylase, a putative virulence factor in *Streptococcus pneumoniae*. *Infect Immun* 2002;70:7176–8.
- [7] Fukushima T, Kitajima T, Sekiguchi J. A polysaccharide deacetylase homologue PdaA, in *Bacillus subtilis* acts as an N-acetylmuramic acid deacetylase in vitro. *J Bacteriol* 2005;187:1287–92.
- [8] Psyllinakis E, Boneca IG, Mavromatis K, Deli A, Hayhurst E, Foster SJ, et al. Peptidoglycan N-acetylglucosamine deacetylases from *Bacillus cereus*, highly conserved proteins in *Bacillus anthracis*. *J Biol Chem* 2005;280:30856–63.
- [9] Meyrand M, Boughammoura A, Courtin P, Mezange C, Guillot A, Chapot-Chartier MP. Peptidoglycan N-acetylglucosamine deacetylation decreases autolysis in *Lactococcus lactis*. *Microbiology* 2007;153:3275–85.
- [10] Deng DM, Urch JE, ten Cate JM, Rao VA, van Aalten DM, Crielgaard W. *Streptococcus mutans* SMU.623c codes for a functional, metal-dependent polysaccharide deacetylase that modulates interactions with salivary agglutinin. *J Bacteriol* 2009;191:394–402.
- [11] Boneca IG, Dussurget O, Cabanes D, Nahori MA, Sousa S, Lecuit M, et al. A critical role for peptidoglycan N-deacetylation in *Listeria* evasion from the host innate immune system. *Proc Natl Acad Sci USA* 2007;104:997–1002.
- [12] Popowska M, Kusio M, Szymanska P, Markiewicz Z. Inactivation of the wall-associated de-N-acetylase (PgdA) of *Listeria monocytogenes* results in greater susceptibility of the cells to induced autolysis. *J Microbiol Biotechnol* 2009;19:932–45.
- [13] Hebert L, Courtin P, Torelli R, Sanguinetti M, Chapot-Chartier MP, Auffray Y, et al. *Enterococcus faecalis* constitutes an unusual bacterial model in lysozyme resistance. *Infection Immunity* 2007;75:5390–8.
- [14] Fittipaldi N, Sekizaki T, Takamatsu D, Dominguez-Punaro Mde L, Harel J, Bui NK, et al. Significant contribution of the pgdA gene to the virulence of *Streptococcus suis*. *Mol Microbiol* 2008;70:1120–35.
- [15] Milani CJ, Aziz RK, Locke JB, Dahesh S, Nizet V, Buchanan JT. The novel polysaccharide deacetylase homologue Pdi contributes to virulence of the aquatic pathogen *Streptococcus iniae*. *Microbiology* 2010;156:543–54.
- [16] Blair DE, Schüttelkopf AW, MacRae JI, van Aalten DM. Structure and metal-dependent mechanism of peptidoglycan deacetylase, a streptococcal virulence factor. *Proc Natl Acad Sci USA* 2005;102:15429–34.
- [17] Garcia-Bustos JF, Tomasz A. Teichoic acid-containing muropeptides from *Streptococcus pneumoniae* as substrates for the pneumococcal autolysin. *J Bacteriol* 1987;169:447–53.
- [18] Glauner B. Separation and quantification of muropeptides with high-performance liquid chromatography. *Anal Biochem* 1988;172:451–64.

- [19] Bui NK, Gray J, Schwarz H, Schumann P, Blanot D, Vollmer W. The peptidoglycan sacculus of *Myxococcus xanthus* has unusual structural features and is degraded during glycerol-induced myxospore development. *J Bacteriol* 2009;191:494–505.
- [20] Lipinski CA, Lombardo F, Dominy BW, Feeney PJ. Experimental and computational approaches to estimate solubility and permeability in drug discovery and development settings. *Adv Drug Del Rev* 2001;46:3–26.
- [21] Shoichet BK. Screening in a spirit haunted world. *Drug Discov Today* 2006;11:607–15.
- [22] Rarey M, Kramer B, Lengauer T, Klebe G. A fast flexible docking method using an incremental construction algorithm. *J Mol Biol* 1996;261:470–89.
- [23] Grant JA, Gallardo MA, Pickup BT. A fast method of molecular shape comparison: a simple application of a Gaussian description of molecular shape. *J Comp Chem* 2006;17:1653–66.
- [24] Tanrikulu Y, Nietert M, Scheffer U, Proschak E, Grabowski K, Schneider P, et al. Scaffold hopping by “fuzzy” pharmacophores and its application to RNA targets. *ChemBioChem* 2007;8:1932–6.
- [25] Ripphausen P, Nisius B, Peltason L, Bajorath J. Quo vadis, virtual screening? A comprehensive survey of prospective applications. *J Med Chem* 2010;53:8461–7.
- [26] Klebe G. Virtual ligand screening: strategies, perspectives and limitations. *Drug Discov Today* 2006;11:580–94.
- [27] Simmons KJ, Chopra I, Fishwick CW. Structure-based discovery of antibacterial drugs. *Nat Rev Microbiol* 2010;8:501–10.